Inorg. Chem. **2009**, *48*, 1301−1308

Diversity of Azido Magnetic Chains Constructed with Flexible Ligand 2,2′-Dipyridylamine

Xiu-Teng Wang, Xiao-Hua Wang, Zhe-Ming Wang, and Song Gao*

Beijing National Laboratory for Molecular Sciences, State Key Laboratory of Rare Earth Materials Chemistry and Applications, College of Chemistry and Molecular Engineering, Peking University, Beijing 100871, P. R. China

Received August 8, 2008

By employing a flexible molecule, 2,2′-dipyridylamine (dpa), as a bidentate coligand, three azide-bridged one-dimensional coordination polymers, $[M(dpa)(N_3)_2]_n$ (M = Cu, **1·Cu**; Co, **2·Co**) and $[Ni(dpa)(OAc)_{0.5}(N_3)_{1.5}(H_2O)]_n$ (**3·Ni**), have been successfully synthesized and structurally and magnetically characterized. They show versatile one-dimensional chain structures. **1·Cu** is an EO-N_3 bridged uniform chain; **2·Co** is an alternative chain linked by two EO-N_3 and two EE-N_3 bridges. Interestingly, **3·Ni** is a zigzag chain linked alternatively by one EE-N_3 and a novel 3-fold bridge, which is composed of two EO-N_3 and one acetate group. This series of azido complexes demonstrates that the flexibility of the dpa ligand plays an important role in directing the structures of the final products. Magnetic studies reveal dominant intrachain antiferromagnetic couplings in compound **1·Cu**. Compounds **2·Co** and **3·Ni** are weak ferromagnets due to the spin canting, with critical temperatures of 12.4 and 32.5 K, respectively.

Introduction

Low-dimensional magnetic coordination polymers have attracted much attention since the discovery of intriguing anisotropic systems with fascinating physical properties, such as single molecule magnets[1] and single-chain magnets.[2] To design 0D or 1D molecule-based magnetic materials with characteristic and tunable properties, it is obviously important to select appropriate bridging ligands to transmit effectively the exchange interactions between the paramagnetic centers. The azide anion (N_3^-) is one of the most extensively employed short bridges[3] due to the virtue of its magnetic predictability and extreme versatile coordination modes [μ_2-1,3 (end-to-end, EE), μ_2-1,1 (end-on, EO), μ_3-1,1,1, μ_3-1,1,3, and other more complicated modes]. Generally, azide bridges can mediate ferromagnetic (FO) couplings in the EO mode and antiferromagnetic (AF) couplings in the EE mode, although several exceptions have been reported.[4] What's more, its diverse binding ability has brought on various discrete clusters,[5] one-dimensional chains,[6] two-dimensional sheets,[7] or three-dimensional networks[8] with the cooperation of appropriate ancillary ligands.

The common strategy for the preparation of 1D coordination polymers has been systematically employed by blocking several coordinate sites of metal ions with terminal ligands

* To whom correspondence should be addressed. Tel.: +86 10 62756320. Fax: +86 10 62751708. E-mail: gaosong@pku.edu.cn.

(1) (a) Caneschi, A.; Gatteschi, D.; Sessoli, R.; Barra, A. L.; Brunel, L. C.; Guillot, M. *J. Am. Chem. Soc.* **1991**, *113*, 5873. (b) Thomas, L.; Lionti, F.; Ballou, R.; Sessoli, R.; Gatteschi, D.; Barbara, B. *Nature* **1996**, *383*, 145. (c) Hill, S.; Edwards, R. S.; Aliaga-Alcalde, N.; Christou, G. *Science* **2003**, *302*, 1015. (d) Sessoli, R.; Gatteschi, D.; Caneschi, A.; Novak, M. A. *Nature* **1993**, *365*, 141. (e) Sessoli, R.; Tsai, H. L.; Schake, A. R.; Wang, S.; Vincent, J. B.; Folting, K.; Gatteschi, D.; Christou, G.; Hendrickson, D. N. *J. Am. Chem. Soc.* **1993**, *115*, 1804.

(2) (a) Gatteschi, D.; Sessoli, R. *Angew. Chem., Int. Ed.* **2003**, *42*, 268. (b) Caneschi, A.; Gatteschi, D.; Lalioti, N.; Sangregorio, C.; Sessoli, R.; Venturi, G.; Vindigni, A.; Rettori, A.; Pini, M. G.; Novak, M. A. *Angew. Chem., Int. Ed.* **2001**, *40*, 1760. (c) Lescouëzec, R.; Toma, L. M.; Vaissermann, J.; Verdaguer, M.; Delgado, F. S.; Ruiz-Pérez, C.; Lloret, F.; Julve, M. *Coord. Chem. Rev.* **2005**, *249*, 2691. (d) Clerac, R.; Miyasaka, H.; Yamashita, M.; Coulon, C. *J. Am. Chem. Soc.* **2002**, *124*, 12837. (e) Liu, T. F.; Fu, D.; Gao, S.; Zhang, Y.-Z.; Sun, H.-L.; Su, G.; Liu, Y. *J. Am. Chem. Soc.* **2003**, *125*, 13976. (f) Xu, H.-B.; Wang, B.-W.; Pan, F.; Wang, Z.-M.; Gao, S. *Angew. Chem., Int. Ed.* **2007**, *46*, 7388.

(3) (a) Kahn, O. *Molecular Magnetism*; VCH: New York, 1993. (b) Miller, J. S.; Drillon, M. *Magnetism: Molecules to Materials*; Wiley-VCH: Weinheim, Germany, 2002. (c) Wang, X.-T.; Wang, Z.-M.; Gao, S. *Inorg. Chem.* **2007**, *46*, 10452. (d) Ribas, J.; Escuer, A.; Monfort, M.; Vicente, R.; Cortes, R.; Lezama, L.; Rojo, T. *Coord. Chem. Rev.* **1999**, *193*−*195*, 1027, and references therein.

(4) (a) For examples: Escuer, A.; Vicente, R.; Mautner, F. A.; Goher, M. A. S.; Abu-Youssef, M. A. M. *Chem. Commun.* **2002**, 64. (b) Blanchet-Boiteux, C.; Mouesca, J.-M. *J. Am. Chem. Soc.* **2000**, *122*, 861. (c) Cui, H.-B.; Wang, Z.-M.; Takahashi, K.; Okano, Y.; Kobayashi, H.-Y.; Kobayashi, A. *J. Am. Chem. Soc.* **2006**, *128*, 15074.

10.1021/ic801505a CCC: $40.75
Published on Web 01/15/2009

Chart 1

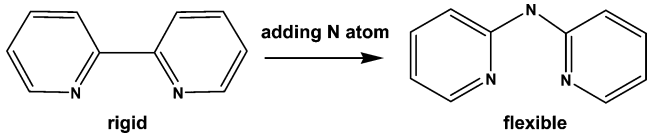

and, meanwhile, linking them through short bridges binding to the left vacancies. For the azide bridge, many rigid organic blocking coligands have been chosen to construct 1D magnetic compounds such as 2,2′-bipyridine (2,2′-bpy),[6c,9] phenanthroline (phen),[10] and 2,2′-bipyrimidine.[11] Due to the steric rigidity of blocking ligands, the structures of these azido compounds are lacking obvious differences.

For example, the complexes $[M(2,2'\text{-bpy})(N_3)_2]_n$ (M = Ni, Co, Fe, and Mn) are all 1D chains linked by two EO and two EE azido bridges alternatively. In view of the coordination chemistry, if we enhance the flexibility of these chelating ligands, more tunable coordination modes and thus more final product topologies can be expected, since the flexibility of the coligands provides extra freedom to the formation of the structures. For instance, if there are one or more groups between the neighboring pyridyl rings of 2,2′-bpy, the two rings will be able to rotate, displaying much more changeable abilities than 2,2′-bpy itself. Herein, following this strategy, we have successfully synthesized three azido complexes by using a more flexible molecule, 2,2′-dipyridylamine (dpa), as the blocking ligand (Chart 1): $[M(dpa)(N_3)_2]_n$ (M = Cu, **1·Cu**; Co, **2·Co**) and $[Ni(dpa)(OAc)_{1/2}(N_3)_{3/2}(H_2O)]_n$ (**3·Ni**). As we anticipated before, different chain structures are obtained. Compound **1·Cu** is a uniform chain bridged by EO-N_3. Compound **2·Co** has alternative chains similar to the transition metal complexes built by 2,2′-bpy. Interestingly, in compound **3·Ni**, the Ni(II) ions are linked alternately by an uncommon 3-fold bridge and an EE-N_3 to form a novel 1D chain. The 3-fold bridges are made up of two EO-N_3 and one acetate group, which are very scarce.[12,13] In the literature, two other azido−dpa complexes, $Mn(dpa)(N_3)_2$ (**4**)[14] and $[Ni(dpa)(N_3)_2]\cdot H_2O$ (**5**),[15] which we have also prepared and characterized, have been reported. When compounds **4** and **5** are taken into account, it is obvious that the dpa-based compounds show a variety of topologies, far from those built with the rigid compounds, such as 2,2′-bpy,[6c,9] phen,[10] and 2,2′-bipyrimidine.[11] This indicates that the flexibility of the blocking ligand has an important impact on the compounds' structures. Magnetic studies suggest that the dominant AF couplings exhibit in compound **1·Cu** no long-range ordering (LRO) above 2.0 K. Compounds **2·Co** and **3·Ni** show weak ferromagnetic behavior due to the spin canting.

Experimental Section

Materials and Apparatus. All chemicals for synthesis were commercially available reagents of analytical grade and were used as purchased without further purification.

Caution! *Although not encountered in our experiments, azido compounds and perchlorate salts of metal ions are potentially explosive and should be manipulated with care and used only in small quantities.*

Elemental analyses (C, H, and N) were performed on an Elementar Vario EL analyzer. The infrared spectra were recorded against pure crystals on a Nicolet Magna-IR 750 spectrometer equipped with a Nic-Plan microscope in the 4000−500 cm^{-1} region.

Synthesis. $[Cu(dpa)(N_3)_2]_n$ (1·Cu). In a test tube, an aqueous solution of $Cu(ClO_4)_2\cdot 6H_2O$ (0.10 M, 6 mL) was layered carefully with 2 mL of tetrahydrofuran and then a mixture of a methanol solution of dpa (0.10 M, 5 mL) and an aqueous solution of NaN_3(2.0 M, 0.50 mL). The tube was sealed and left undisturbed at room temperature. X-ray-quality black needle crystals appeared five days later in a yield of 57% based on $Cu(ClO_4)_2\cdot 6H_2O$. Anal. calcd for **1·Cu**, $CuC_{10}H_9N_9$: C, 37.68; H, 2.85; N, 39.54. Found: C, 37.65; H, 2.89; N, 39.49. IR bands (cm^{-1}): 3342w, 2082vs, 2036vs, 1635m, 1590m, 1527m, 1481s, 1434w, 1415w, 1234m, 1166m, 1016m, 910w, 761m.

$[Co(dpa)(N_3)_2]_n$ (2·Co). A similar procedure to that for **1·Cu** was employed using $Co(ClO_4)_2\cdot 6H_2O$ instead of $Cu(ClO_4)_2\cdot 6H_2O$. Dark red block crystals were obtained after two weeks with a yield of 52% based on $Co(ClO_4)_2\cdot 6H_2O$. Anal. calcd for **2·Co**, $CoC_{10}H_9N_9$: C, 38.23; H, 2.89; N, 40.12. Found: C, 38.20; H, 2.96;

(5) (a) Serna, Z. E.; Lezama, L.; Urtiaga, M. K.; Arriortua, M. I.; Barandika, M. G.; Cortés, R.; Rojo, T. *Angew. Chem., Int. Ed.* **2000**, *39*, 344. (b) Papaefstathiou, G. S.; Perlepes, S. P.; Escuer, A.; Vicente, R.; Font-Bardia, M.; Solans, X. *Angew. Chem., Int. Ed.* **2001**, *40*, 884. (c) Dendrinou-Samara, C.; Alexiou, M.; Zaleski, C. M.; Kampf, J. W.; Kirk, M. L.; Kessissoglou, D. P.; Pecoraro, V. L. *Angew. Chem., Int. Ed.* **2003**, *42*, 3763. (d) Zhang, Y.-Z.; Wernsdorfer, W.; Pan, F.; Wang, Z.-M.; Gao, S. *Chem. Commun.* **2006**, 3302. (e) Yang, C.-I.; Wernsdorfer, W.; Lee, G.-H.; Tsai, H.-L. *J. Am. Chem. Soc.* **2007**, *129*, 456.

(6) (a) Hong, C. S.; Do, Y. *Angew. Chem., Int. Ed.* **1999**, *38*, 193. (b) Liu, X. T.; Wang, X. Y.; Zhang, W. X.; Cui, P.; Gao, S. *Adv. Mater.* **2006**, *18*, 2852. (c) Cortés, R.; Drillon, M.; Solans, X.; Lezama, L.; Rojo, T. *Inorg. Chem.* **1997**, *36*, 677.

(7) (a) Wang, X.-Y.; Wang, L.; Wang, Z.-M.; Su, G.; Gao, S. *Chem. Mater.* **2005**, *17*, 6369. (b) Gao, E.-Q.; Yue, Y.-F.; Bai, S.-Q.; He, Z.; Yan, C.-H. *J. Am. Chem. Soc.* **2004**, *126*, 1419. (c) You, Y. S.; Yoon, J. H.; Kim, H. C.; Hong, C. S. *Chem. Commun.* **2005**, 4116.

(8) (a) Goher, M. A. S.; Cano, J.; Journaux, Y.; Abu-Youssef, M. A. M.; Mautner, F. A.; Escuer, A.; Vicente, R. *Chem.—Eur. J.* **2000**, *6*, 778. (b) Wang, X.-Y.; Wang, L.; Wang, Z.-M.; Gao, S. *J. Am. Chem. Soc.* **2006**, *128*, 674. (c) Martín, S.; Barandika, M. G.; Lezama, L.; Pizarro, J. L.; Serna, Z. E.; Ruiz de Larramendi, J. I.; Arriortua, M. I.; Rojo, T.; Cortés, R. *Inorg. Chem.* **2001**, *40*, 4109.

(9) (a) Wen, H.-R.; Zuo, J.-L.; Liu, W.; Song, Y.; You, X.-Z. *Inorg. Chim. Acta* **2005**, *358*, 2565. (b) Cortés, R.; Lezama, L.; Pizarro, J. L.; Arriortua, M. I.; Solans, X.; Rojo, T. *Angew. Chem., Int. Ed.* **1994**, *33*, 2488. (c) Viau, G.; Lombardi, M. G.; Munno, G. D.; Julve, M.; Lloret-Juan, F. *Chem. Commun.* **1997**, 1195.

(10) (a) Liu, F.-C.; Zeng, Y.-F.; Zhao, J.-P.; Hu, B.-W.; Bu, X.-H.; Ribas, J.; Cano, J. *Inorg. Chem.* **2007**, *46*, 1520. (b) Liang, M.; Wang, W. Z.; Liu, Z. Q.; Liao, D. Z.; Jiang, Z. H.; Yan, S. P.; Cheng, P. *J. Cood. Chem.* **2003**, *56*, 1473. (c) Konar, S.; Zangrando, E; Drew, M. G. B.; Mallah, T.; Ribas, J.; Chaudhuri, N. R. *Inorg. Chem.* **2003**, *42*, 5966.

(11) (a) De Munno, G.; Julve, M.; Viau, G.; Lloret, F.; Faus, J.; Viterbo, D. *Angew. Chem., Int. Ed.* **1996**, *35*, 1807. (b) Cortés, R.; Lezama, L.; Pizarro, J. L.; Arriortua, M. I.; Fojo, T. *Angew. Chem., Int. Ed.* **1996**, *35*, 1810. (c) De Munno, G.; Poerio, T.; Viau, G.; Julve, M.; Lloret, F.; Journaux, Y.; Rivière, E. *Chem. Commun.* **1996**, 2587.

(12) Ribas, J.; Monfort, M.; Ghosh, B. K.; Solans, X. *Angew. Chem., Int. Ed.* **1994**, *33*, 2087.

(13) (a) Han, Y.-F.; Wang, T.-W.; Song, Y.; Shen, Z.; You, X.-Z. *Inorg. Chem. Commun.* **2008**, *11*, 207. (b) Liu, T.; Zhang, Y.-J.; Wang, Z.-M.; Gao, S. *Inorg. Chem.* **2006**, *45*, 2782.

(14) Villanueva, M.; Mesa, J. L.; Urtiaga, M. K.; Cortés, R.; Lezama, L.; Arriortua, M. I.; Rojo, T. *Eur. J. Inorg. Chem.* **2001**, 1581.

(15) Yu, X.; You, W.; Guo, X.; Zhang, L.; Xu, Y.; Sun, Z.; Clérac, R. *Inorg. Chem. Commun.* **2007**, *10*, 1335.

N, 40.19. IR bands (cm^{-1}): 3320w, 3216w, 3043w, 2086vs, 2051vs, 1643m, 1585m, 1535m, 1481m, 1432m, 1423m, 1384w, 1349w, 1295w, 1234m, 1157m, 1010m, 914w, 833w, 761m.

$[Ni(OAc)_{1/2}(N_3)_{3/2}(H_2O)]_n$ (3·Ni). A similar procedure to that for **1·Cu** was employed using $Ni(OAc)_2 \cdot 4H_2O$ instead of $Cu(ClO_4)_2 \cdot 6H_2O$. Blue block crystals were obtained after three weeks with a yield of 38% based on $Ni(OAc)_2 \cdot 4H_2O$. Anal. calcd for **3·Ni**, $NiC_{11}H_{12.5}N_{7.5}O_2$: C, 38.81; H, 3.70; N, 30.86. Found: C, 38.78; H, 3.76; N, 30.82. IR bands (cm^{-1}): 3329w, 3203w, 3139w, 3089w, 2082s (sh), 2063vs, 1637m, 1585m, 1565m, 1475m, 1434m, 1417m, 1363m, 1236m, 1155m, 1014m, 769m.

X-Ray Crystallography. Crystallographic data for the single crystals of **1·Cu**, **2·Co**, and **3·Ni** were collected on a Nonius Kappa CCD diffractometer equipped with graphite monochromated Mo Kα radiation of $\lambda = 0.71073$ Å.[16] Empirical absorption corrections were applied using the Sortav program.[17] All of the structures were solved using the direct method and refined using the full-matrix least-squares method on F^2 with anisotropic thermal parameters for all non-hydrogen atoms using the SHELX program.[18] Hydrogen atoms of the lattice water were not included. Other hydrogen atoms were added by calculation positions. The powder X-ray diffraction pattern for compound **2·Co** was obtained on a Rigaku D/max 2000 diffractometer at room temperature with Cu Kα radiation in flat plate geometry.

Magnetic Properties. The magnetic measurements of the three compounds for polycrystalline samples were performed on a Quantum Design MPMS XL-5 SQUID system in the temperatures range 2.0−300 K. The isothermal magnetizations were measured with an applied field from −50 to +50 kOe. The ac measurements were performed at various frequencies from 1 to 1000 Hz with an ac field amplitude of 3 Oe under zero dc field. Magnetic data were corrected for the diamagnetic contribution calculated from Pascal constants[3a] and a background of the sample holder.

Results and Discussion

Synthesis and IR Spectra. Compounds **1·Cu**, **2·Co**, and **3·Ni** were all synthesized through slow diffusions because mixing the corresponding reactants would quickly bring on a large amount of precipitate. Compound **3·Ni**, which contains a novel triple bridge (see the following Crystal Structures section for detailed discussion), was obtained by using $Ni(OAc)_2 \cdot 4H_2O$ as a Ni^{2+} source. We tried to acquire similar structures of $OAc/(N_3)_2$ triple bridges based on Mn(II), Co(II), and Cu(II) without success, which may indicate that only the radius of the Ni^{2+} ion is suitable for an acetate group to form these triple bridges. We also attempted to introduce a formate group ($HCOO^-$) into the reaction systems with metal formate salts, thus obtaining possible bridges similar to compound **3·Ni**, but just the same compounds as those using perchlorates were isolated. These experiments demonstrate the important influence of anion bridging ligands on the product topologies, even for acetate and formate groups.

Table 1. Crystal Data and Structure Determination Summaries for **1·Cu**−**3·Ni**

	1·Cu	**2·Co**	**3·Ni**
formula	$CuC_{10}H_9N_9$	$CoC_{10}H_9N_9$	$NiC_{11}H_{12.5}N_{7.5}O_2$
fw	318.79	314.17	340.46
cryst syst	monoclinic	monoclinic	triclinic
space group	$P2_1/c$	$P2_1/n$	$P\bar{1}$
a [Å]	9.1030(5)	9.4540(19)	8.4022(2)
b [Å]	18.4793(7)	7.3571(15)	11.6981(3)
c [Å]	7.0560(3)	17.9903(4)	15.2421(4)
α [deg]	90	90	95.0084(9)
β [deg]	92.287(2)	99.885(6)	97.6127(9)
γ [deg]	90	90	103.9581(9)
V [Å^3]	1185.99(9)	1232.7(4)	1429.97(6)
Z	4	4	4
ρ_{calcd} [g cm^{-3}]	1.785	1.693	1.582
$F(000)$	644	636	700
cryst size [mm]	0.16 × 0.15 × 0.12	0.30 × 0.27 × 0.12	0.47 × 0.27 × 0.20
T [K]	293(2)	293(2)	293(2)
θ_{limit} [deg]	3.64−24.97	3.53−25.04	3.395−26.373
collected reflns	18020	17473	29873
unique reflns	2074	2178	5838
R_{int}	0.1054	0.0559	0.0617
T_{max}/T_{min}	0.878 − 0.777	0.850 − 0.739	0.765 − 0.652
no. of params	2074/0/181	2178/0/181	5838/0/388
GOF	0.911	1.011	1.003
R_1[a]	0.0322	0.0275	0.0345
wR_2[b]	0.0585	0.0634	0.0846

[a] $R_1 = \sum ||F_o| - |F_c|| / \sum |F_o|$. [b] $wR_2 = [\sum w(F_o^2 - F_c^2)^2 / \sum w(F_o^2)^2]^{1/2}$.

Table 2. Selected Bond Lengths (Å) and Angles (deg) for Complex **1·Cu**

Cu(1)−N(7)	1.961(3)	N(4)−Cu(1)[a]	2.030(2)
Cu(1)−N(3)	1.994(2)	N(4)−N(5)	1.205(3)
Cu(1)−N(4)[b]	2.030(2)	N(5)−N(6)	1.152(4)
Cu(1)−N(1)	2.043(2)	N(8)−N(9)	1.160(3)
Cu(1)−N(4)	2.370(2)	N(8)−N(7)	1.190(3)
N(7)−Cu(1)−N(3)	174.37(11)	N(4)[b]−Cu(1)−N(4)	107.52(9)
N(7)−Cu(1)−N(4)[b]	92.14(11)	N(1)−Cu(1)−N(4)	108.31(9)
N(3)−Cu(1)−N(4)[b]	88.62(10)	N(5)−N(4)−Cu(1)[a]	118.96(19)
N(7)−Cu(1)−N(1)	93.04(11)	N(5)−N(4)−Cu(1)	115.95(18)
N(3)−Cu(1)−N(1)	89.61(10)	Cu(1)[a]−N(4)−Cu(1)	124.11(12)
N(4)[b]−Cu(1)−N(1)	144.01(10)	N(6)−N(5)−N(4)	178.6(3)
N(7)−Cu(1)−N(4)	86.92(10)	N(9)−N(8)−N(7)	177.7(3)
N(3)−Cu(1)−N(4)	87.53(9)	N(8)−N(7)−Cu(1)	124.4(2)

[a] Symmetry operation: x, $-y + 1/2$, $z - 1/2$. [b] Symmetry operation: x, $-y + 1/2$, $z + 1/2$.

The IR spectra of the complexes display characteristic bands of the azide on the basis of their bridging modes. In the region expected for the ν_{as}-(N_3) absorption, compounds **1·Cu** and **2·Co** exhibit two well-separated neighboring sharp and strong bands in the 2100∼2030 cm^{-1} range, attributable to the presence of two kinds of bridging modes of azide (EE- and EO-N_3) in the compounds. For **3·Ni**, a very strong band in the 2070∼2060 cm^{-1} range with a shoulder peak is observed, suggesting the presence of different bridging modes of azide. The two medium absorptions of **3·Ni** at ca. 1565 and 1475 cm^{-1} are assignable to the $\nu_{as}(CH_3COO)$ and $\nu_s(CH_3COO)$ modes of the acetate bridge.

Crystal Structures. The crystallographic and refinement details of these three compounds are summarized in Table 1. The selected bond lengths and angles are listed in Tables 2−4. Compound **1·Cu** is a uniform chain bridged by a single EO-N_3, with another N_3 as the terminal ligand. Compound **2·Co** consists of linear neutral chains alternatively bridged by double EO-N_3 and double EE-N_3. Compound **3·Ni** is also a Ni(II) chain connected by one EE-N_3 and one 3-fold bridges in alternation, in which the 3-fold bridge consists of one

(16) (a) *Collect*; Nonius BV: Delft, The Netherlands, 1998. (b) *HKL2000*; *maXus*; University of Glasgow: Glasgow, Scotland, U. K.; Nonius BV: Delft, The Netherlands; MacScience Co. Ltd.: Yokohama, Japan, 2000.

(17) (a) Blessing, R. H. *Acta Crystallogr., Sect. A* **1995**, *51*, 33. (b) Blessing, R. H. *J. Appl. Crystallogr.* **1997**, *30*, 421.

(18) (a) Sheldrick, G. M. *SHELXTL*, version 5.1; Bruker Analytical X-ray Instruments Inc.: Madison, WI, 1998. (b) Sheldrick, G. M. *SHELX-97*, PC Version; University of Göttingen: Göttingen, Germany, 1997.

Table 3. Selected Bond Lengths (Å) and Angles (deg) for Complex **2·Co**

Co(1)−N(3)	2.1128(18)	N(4)−N(5)	1.188(2)
Co(1)−N(7)	2.130(2)	N(4)−Co(1)^a	2.1712(18)
Co(1)−N(1)	2.1305(17)	N(5)−N(6)	1.152(3)
Co(1)−N(4)	2.1599(18)	N(7)−N(8)	1.162(2)
Co(1)−N(9)^b	2.163(2)	N(8)−N(9)	1.171(3)
Co(1)−N(4)^a	2.1712(19)	N(9)−Co(1)^b	2.163(2)
N(3)−Co(1)−N(7)	91.12(8)	N(7)−Co(1)−N(4)^a	90.54(7)
N(3)−Co(1)−N(1)	87.17(7)	N(1)−Co(1)−N(4)^a	100.39(7)
N(7)−Co(1)−N(1)	168.99(7)	N(4)−Co(1)−N(4)^a	76.30(8)
N(3)−Co(1)−N(4)	168.60(7)	N(9)a−Co(1)−N(4)^a	173.74(7)
N(7)−Co(1)−N(4)	87.89(8)	N(5)−N(4)−Co(1)	126.69(15)
N(1)−Co(1)−N(4)	95.90(7)	N(5)−N(4)−Co(1)^a	128.34(15)
N(3)−Co(1)−N(9)^b	93.63(7)	Co(1)−N(4)−Co(1)^a	103.70(8)
N(7)−Co(1)−N(9)^b	87.49(8)	N(6)−N(5)−N(4)	179.7(3)
N(1)−Co(1)−N(9)^b	81.77(7)	N(8)−N(7)−Co(1)	134.96(16)
N(4)−Co(1)−N(9)^b	97.67(8)	N(7)−N(8)−N(9)	176.7(2)
N(3)−Co(1)−N(4)^a	92.35(7)	N(8)−N(9)−Co(1)^b	128.74(15)

^{a} Symmetry operation: $-x+1, -y+2, -z+1$. ^{b} Symmetry operation: $-x+1, -y+1, -z+1$.

Table 4. Selected Bond Lengths (Å) and Angles (deg) for Complex **3·Ni**

Ni(1)−O(2)	2.0226(18)	Ni(2)−N(7)	2.117(2)
Ni(1)−N(1)	2.058(2)	Ni(2)−N(15)^a	2.121(2)
Ni(1)−N(3)	2.060(2)	N(8)−N(9)	1.156(3)
Ni(1)−N(13)	2.071(2)	N(8)−N(7)	1.185(3)
Ni(1)−N(10)	2.125(2)	N(10)−N(11)	1.197(3)
Ni(1)−N(7)	2.142(2)	N(11)−N(12)	1.153(3)
Ni(2)−O(1)	2.0490(18)	N(13)−N(14)	1.163(3)
Ni(2)−N(6)	2.070(2)	N(14)−N(15)	1.180(3)
Ni(2)−N(4)	2.085(2)	N(15)−Ni(2)^b	2.121(2)
Ni(2)−N(10)	2.107(2)		
O(2)−Ni(1)−N(1)	177.74(8)	O(1)−Ni(2)−N(7)	90.27(8)
O(2)−Ni(1)−N(3)	91.49(8)	N(6)−Ni(2)−N(7)	97.29(8)
N(1)−Ni(1)−N(3)	86.31(9)	N(4)−Ni(2)−N(7)	91.53(8)
O(2)−Ni(1)−N(13)	90.34(9)	N(10)−Ni(2)−N(7)	79.74(8)
N(1)−Ni(1)−N(13)	89.36(9)	O(1)−Ni(2)−N(15)^a	89.10(8)
N(3)−Ni(1)−N(13)	95.30(10)	N(6)−Ni(2)−N(15)^a	92.84(8)
O(2)−Ni(1)−N(10)	90.75(8)	N(4)−Ni(2)−N(15)^a	89.41(8)
N(1)−Ni(1)−N(10)	89.80(8)	N(10)−Ni(2)−N(15)^a	90.13(9)
N(3)−Ni(1)−N(10)	91.28(9)	N(7)−Ni(2)−N(15)^a	169.86(9)
N(13)−Ni(1)−N(10)	173.30(10)	N(9)−N(8)−N(7)	178.9(3)
O(2)−Ni(1)−N(7)	88.82(8)	N(11)−N(10)−Ni(2)	120.79(18)
N(1)−Ni(1)−N(7)	93.43(8)	N(11)−N(10)−Ni(1)	120.66(18)
N(3)−Ni(1)−N(7)	170.03(8)	Ni(2)−N(10)−Ni(1)	97.79(8)
N(13)−Ni(1)−N(7)	94.66(9)	N(12)−N(11)−N(10)	178.9(3)
N(10)−Ni(1)−N(7)	78.76(8)	N(8)−N(7)−Ni(2)	131.92(18)
O(1)−Ni(2)−N(6)	90.70(8)	N(8)−N(7)−Ni(1)	129.04(17)
O(1)−Ni(2)−N(4)	177.58(8)	Ni(2)−N(7)−Ni(1)	96.95(8)
N(6)−Ni(2)−N(4)	87.46(8)	N(14)−N(13)−Ni(1)	139.3(2)
O(1)−Ni(2)−N(10)	88.24(8)	N(13)−N(14)−N(15)	178.5(3)
N(6)−Ni(2)−N(10)	176.84(8)	N(14)−N(15)−Ni(2)^b	124.41(18)
N(4)−Ni(2)−N(10)	93.67(8)		

^{a} Symmetry operation: $x-1, y, z$. ^{b} Symmetry operation: $x+1, y, z$.

acetate group and two EO-N_3's. More structural details concerning the specific compounds are discussed below.

Structure of Compound 1·Cu. Compound **1·Cu** is composed of a uniform neutral chain in which the Cu(II) ions are bridged by one EO-N_3 with an extra terminal azide ligand (Figure 1 and Figure S1, Supporting Information). Each Cu(II) atom in complex **1·Cu** is penta-coordinated with a distorted trigonal bipyramid geometry. Two nitrogen atoms (N4 and N4 #1, symmetry code #1 = $x, -y+1/2, z+1/2$) of the bridging azide and a nitrogen donor (N1) of the dpa ligand comprise the basal plane, and the axial coordination sites are occupied by one nitrogen atom (N7) of the terminal azide group and the remaining nitrogen atom (N3) of dpa. The bridging EO azido anions are bound asymmetrically to

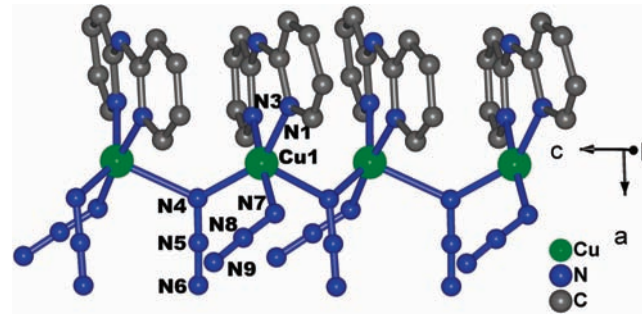

Figure 1. The uniform EO-N_3 bridged chain of **1·Cu** with the atom-labeling scheme (hydrogen atoms are omitted for clarity).

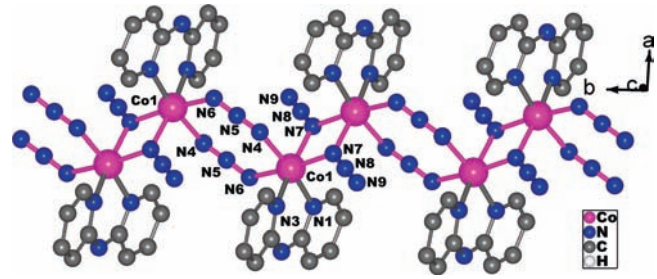

Figure 2. The azido−Co(II) alternative chain of **2·Co** bridged by double EO-N_3 and EE-N_3 with the atom label (H atoms omitted for clarity).

Cu(II) with Cu−N distances of 2.030 and 2.371 Å, and the Cu−N_3−Cu angle is 124.11°. The intrachain Cu···Cu distance is 3.890 Å, which is rather large compared to that observed in Cu(II) compounds with azido anions bridging in an EO mode at the two equatorial positions.[19] The EO azido bridge and the terminal azide are almost linear, with bond angles of ∠N4−N5−N6 = 178.6° and ∠N7−N8−N9 = 178.3°. The bond lengths of N4−N5, N5−N6, N7−N8, and N8−N9 (1.203, 1.147, 1.182, and 1.157 Å, respectively) are approximately equal to each other, and the longer bonds involving the nitrogen atom are linked to the Cu(II) ions. This is consistent with the structural results obtained with the other EO azido bridging complexes.[19]

Structure of Compound 2·Co. The crystal structure of compound **2·Co** (Figure 2) consists of an azido−Co(II) neutral chain with alternative double EO-N_3 and double EE-N_3 bridges, crystallizing in the monoclinic space group $P2_1/n$. There is only one crystallographically independent Co^{2+} ion, which has a distorted octahedral coordination, completed by the two nitrogen atoms of the dpa ligand [Co1−N1 = 2.130 Å, Co1−N3 = 2.113 Å], two nitrogen atoms of EE-N_3 (Co1−N7 = 2.130 Å, Co1−N9#1 = 2.163 Å; symmetry code #1 = $-x+1, -y+1, -z+1$), and two nitrogen atoms of EO-N_3 (Co1−N4 = 2.160 Å, Co1−N4#2 = 2.171 Å; symmetry code #2 = $-x+1, -y+2, -z+1$). Both Co−N bond distances lie in the range of values reported for

(19) (a) Liu, G.-F.; Ren, Z.-G.; Li, H.-X.; Chen, Y.; Li, Q.-H.; Zhang, Y.; Lang, J.-P. *Eur. J. Inorg. Chem.* **2007**, 5511. (b) Stamatatos, T. C.; Papaefstathiou, G. S.; MacGillivray, L. R.; Escuer, A.; Vicente, R.; Ruiz, E.; Perlepes, S. P. *Inorg. Chem.* **2007**, *46*, 8843. (c) Gu, Z.-G.; Zuo, J.-L.; You, X.-Z. *Dalton Trans.* **2007**, 4067. (d) Zhang, Y.-Z.; Wei, H.-Y.; Pan, F.; Wang, Z.-M.; Chen, Z.-D.; Gao, S. *Angew. Chem., Int. Ed.* **2005**, *44*, 5841. (e) Mukherjee, P. S.; Maji, T. K.; Mostafa, G.; Mallah, T.; Chaudhuri, N. R. *Inorg. Chem.* **2000**, *39*, 5147.

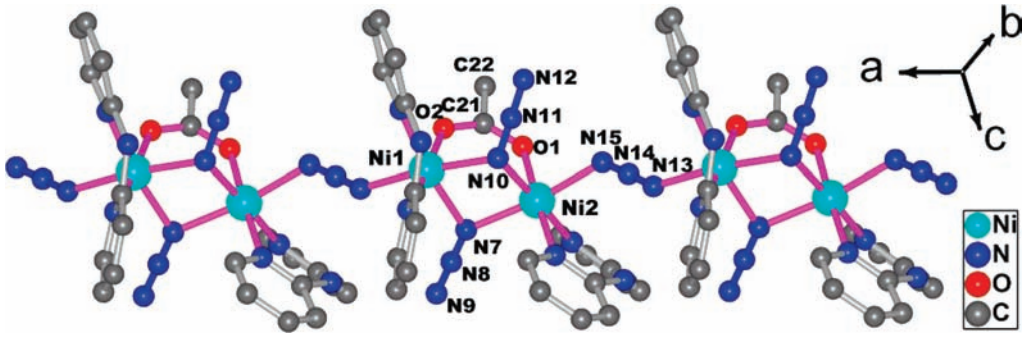

Figure 3. The 1D chain structure of **3·Ni** along the *a* axis (H atoms omitted for clarity) with the atom labeling scheme.

the Co-pyridine ring[8b,9] and Co-azido[20] compounds. The cis N−Co−N angles range from 76.30 to 95.90°, while trans ones range from 168.6 to 173.7°. The existence of an inversion center induces the Co1−N4−Co1#2−N4#2 bridging unit to form a plane, and the EO bridging azides, which are nearly linear (∠N4−N5−N6 = 179.7°), slightly deviate (up and down) from that plane. The Co1−N4−Co1#1 angle in the EO mode is 103.7°, as is usually observed for this kind of bridging. For the EE-N_3 bridges, the Co1−N7−N8 angle is 135.0° and, the Co1#1−N9−N8 angle is 128.8°, for a chair configuration of the Co1−(EE-N3)2−Co1#1 unit and a torsion angle of 36.0°. The intrachain Co···Co distances are 3.407 and 5.366 Å through the EO and EE bridges, respectively. The dpa ligands stack parallel to each other (see Figure S2, Supporting Information) along the chain, which allows the existence of $\pi-\pi$ interactions. The alternative chains pack through the $\pi-\pi$ stacking and H bonds, forming the 3D structure with an interchain Co···Co separation of 9.294 Å.

Structure of Compound 3·Ni. Complex **3·Ni** crystallizes in the triclinic space group $P\bar{1}$. The crystal structure of **3·Ni** is composed of an Ni(II)−azido chain where the metal ions are linked by a 3-fold bridge of one syn−syn acetate and two EO-N_3's, and one EE-N_3 alternatively (Figure 3). Compound **5** also contains another type of windmill-like 3-fold bridge, but it consists of three EO-N_3 bridges (Figure S5, Supporting Information). Moreover, if the triple-bridged dimers are viewed as a node, the EE-N_3 bridges locate in the trans positions of the nodes, and consequently a zigzag Ni(II) chain is obtained. The two unique Ni(II) atoms are in distorted octahedral geometries, coordinated by the N_5O_1 donor atoms, in which the O atom is from the syn−syn bridging acetate ligand and the five N atoms are from dpa, two EO-N_3, and one EE-N_3 ion. The Ni−N distances range from 2.058 to 2.142 Å and the Ni−O distances from 2.023 to 2.049 Å. In the 3-fold bridged dimer, the Ni1−$N_{EO\text{-}azido}$−Ni1#1 (symmetry code #1 = x, $-y + 3/2$, z) angles are 96.87 and 97.73°, larger than those in compound **5**, which is caused by the replacement of one monatomic coordinated azide with an diatomic coordinated acetate group. The presence of an acetate group in the 3-fold bridges results in the elongation of the Ni···Ni distance within the dimer, which is 3.189 Å, longer than that in compound **5** (2.931 Å). Between the dimers, the torsion angle Ni1−(EE-N_3)−Ni2 is 175.3°, with a Ni−N−N angle of 124.43 and 139.08°. The intrachain Ni···Ni separation through EE-N_3 is 5.970 Å. The one-dimensional chains assemble a 3D suparmolecular network through the $\pi-\pi$ interaction of the pyridyl rings of dpa and the O−H_{water}···$N_{EO\ azido}$ and O−H_{water}···$N2_{dpa}$ hydrogen bonds between the chains (Figure S3 of the Supporting Information). The interchain Ni···Ni separation is 7.971 Å.

Table 5. The C−N−C Angles (θ) and the Dihedral Angels (φ) of the Two Pyridyl Rings Observed in the Crystal Structures for **1·Cu**−**3·Ni**

compound	θ/deg	φ/deg
1·Cu	130.58	14.85
2·Co	132.25	10.10
3·Ni	129.58	27.26, 27.02[a]
4	133.83	6.05
5	130.64	28.37

[a] Two crystallographically independent pyridyl rings

Considering the three complexes in this work and the other two compounds **4** (Figure S4, Supporting Information) and **5** (Figure S5, Supporting Information), it is noted that the dpa-based azido complexes are of diverse topologies: a uniform chain, alternating chains, and chains containing 3-fold bridges. On the contrary, the structures of complexes based on 2,2′-bpy and azide, $[M(bpy)(N_3)_2]_n$ (M = Ni(II), Co(II), Fe(II), Mn(II)),[6c,9] are similar to one another. All of them are made up of alternative chains where the metal ions are linked by two EO and two EE azido bridges. The steric arrangement of 2,2′-bpy nearly does not change within the crystal structures of $[M(bpy)(N_3)_2]_n$, and the two pyridyl rings of 2,2′-bpy are almost coplanar. A lack of flexibility of the ligand results in the structural similarity of the complexes with 2,2′-bpy. Different from 2,2′-bpy or phen, the two pyridyl rings of dpa are linked by one nitrogen atom, and they could rotate around the C−N bonds. Additionally, the py−N−py angle (θ) is changeable. At room temperature, the θ angles of dpa in the crystal structures of these complexes range quite wide from 129.6 to 133.8°. The dihedral angels of the two pyridyl rings (φ) range from 6.05 to 28.37° (Table 5). Because the stereo conformation of the dpa ligand has such variability, different types of chain structures are possible, depending on the other factors such as the coordination characteristics of metal ions and short ligands of azido and acetate. This series of compounds demonstrates that employment of a flexible ligand is a useful

(20) (a) Papaefstathiou, G. S.; Escuer, A.; Raptopoulou, C. P.; Terzis, A.; Perlepes, S. P.; Vicente, R. *Eur. J. Inorg. Chem.* **2001**, 1567. (b) Wang, L.-Y.; Zhao, B.; Zhang, C.-X.; Liao, D.-Z.; Jiang, Z.-H.; Yan, S.-P. *Inorg. Chem.* **2003**, *42*, 5804.

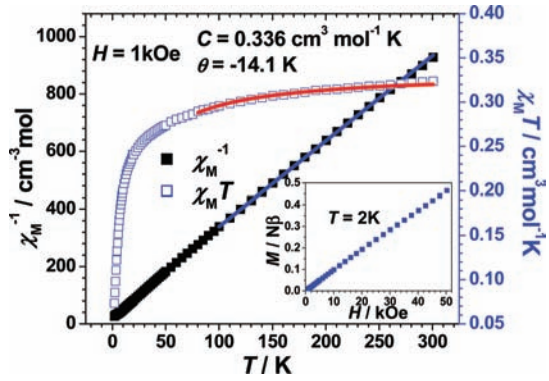

Figure 4. Temperature dependency of $\chi_M T$ and χ_M^{-1} for **1·Cu** at $H = 1$ kOe from 2.0 to 300 K. Inset: Field-dependency of magnetization of **1·Cu** at 2.0 K. The blue solid line represents the best fit to the Curie−Weiss law, and the red one is the fit to the model mentioned in the text.

approach to obtain versatile structures in view of coordination chemistry.

Magnetic Studies. On the basis of the 1D structures mentioned above, it is reasonably expected that the intrachain magnetic coupling via the azido (and the syn−syn acetate for **3·Ni**) bridges is strong, while the interchain ones via $\pi-\pi$ stacking of ligands and hydrogen bonds are weak. In general, in compound **1·Cu**, AF interactions among metal ions are observed; however, no LRO was observed above 2.0 K. Compounds **2·Co** and **3·Ni** are spin-canted weak ferromagnets with $T_N = 12.4$ and 32.5 K, respectively. For **3·Ni**, the structural changes which are caused by the embedment of the acetate group result in the widely different magnetic properties of the two compounds. The details are discussed subsequently below.

1·Cu. The magnetic properties of complex **1·Cu** are shown in Figure 4. The temperature dependence of magnetic susceptibility from 2.0 to 300 K was measured at a 1 kOe field. The $\chi_M T$ value at room temperature is 0.324 cm^3 mol^{-1} K, slightly lower than the theoretical value of spin-only Cu(II) ions (0.375 cm^3 mol^{-1} K). On cooling, the χ_M value increases continuously and reaches 0.0367 cm^3 mol^{-1} at 2.0 K. But the $\chi_M T$ value decreases continuously from 300 K down to 2.0 K, reaching 0.073 cm^3 mol^{-1} K at 2.0 K, indicating the presence of an AF coupling. The value of χ_M above 100 K obeys the Curie−Weiss law, $\chi_M = C/(T - \theta)$, with a Curie constant $C = 0.336$ cm^3 mol^{-1} K and a Weiss constant $\theta = -14.1$ K. For the isotropic Heisenberg antiferromagnet for an $S = 1/2$ system, the molar susceptibility can be expressed as follows based on $H = -2JS_1S_2$:[21]

$$\chi = \frac{Ng^2\beta^2}{kT}\frac{0.25 + 0.074975u + 0.075235u^2}{1.0 + 0.9931u + 0.172135u^2 + 0.757825u^3} \quad (1)$$

where $u = |2J|/kT$. The best fitting for the data from 80 to 300 K gives $J = -3.37$ cm^{-1}, $g = 1.90$ with $R = 2.7 \times 10^{-6}$, and $R = [\sum(\chi_{obsd} - \chi_{calcd})^2/\sum(\chi_{obsd})^2$. The negative θ and J values suggest an AF interaction between the Cu^{2+} ions through the single EO-N_3, which is consistent with the literature reported empirically and theoretically.[22] Thompson et al. have already reported, by comparing the magnetic behavior of several EO-N_3 bridged Cu(II) complexes, the nature of the exchange interaction's change from ferromagnetic to antiferromagnetic when the Cu−N−Cu angle is around 108°.[23] The interaction is found to be ferromagnetic for lower angle values and antiferromagnetic for higher angle values. This empirical conclusion was also confirmed by a density functional study on an EO azido-bridged Cu(II) binuclear model complex,[24] in which the critical Cu−N−Cu angle was found to be 104°. Here, for **1·Cu**, it is clear that the AF interaction results from the large Cu−N−Cu angle (124.11°), much larger than the critical value of 108°.

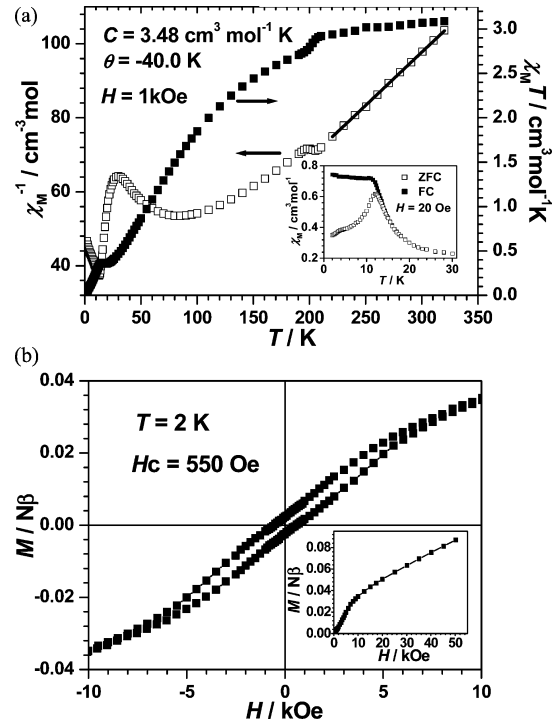

Figure 5. (a) The plots of $\chi_M T$ and χ_M^{-1} vs T for **2·Co** at $H = 1$ kOe from 2.0 to 300 K. Inset: The ZFC−FC plot of **2·Co** at 20 Oe. The solid line represents the best fit to the Curie−Weiss law. (b) The hysteresis of at 2.0 K. Inset: The $M-H$ plot at 2.0 K.

2·Co. Temperature dependencies of the molar magnetic susceptibility χ_M of **2·Co** are presented in Figure 5. The $\chi_M T$ value of ca. 3.07 cm^3 mol^{-1} K at room temperature is much higher than the spin-only value of high-spin d^7 ions (1.87 cm^3 mol^{-1} K), owing to the significant orbital contributions of the distorted octahedral Co^{2+} ions. On lowering the temperature, the $\chi_M T$ values of **2·Co** decrease gradually. Careful inspection of Figure 5a revealed a small turn in the plots of $\chi_M T$ and χ_M^{-1} around 203 K. The experimental powder XRD pattern is consistent with that simulated from the single-crystal structure (Figure S6, Supporting Information), which indicates that the sample is pure. Single-crystal X-ray diffraction measurements show that the structures of

(21) Estes, W. E.; Gaval, D. P.; Hatfield, W. E.; Hodgson, D. *Inorg. Chem.* **1978**, *17*, 1415.
(22) Escuer, A.; Vicente, R.; Mautner, F. A.; Goher, M. A. S. *Inorg. Chem.* **1997**, *36*, 1233.
(23) Tandon, S. S.; Thompson, L. K.; Manuel, M. E.; Bridson, J. N. *Inorg. Chem.* **1994**, *33*, 5555.
(24) Ruiz, E.; Cano, J.; Alvarez, S.; Alemany, P. *J. Am. Chem. Soc.* **1998**, *120*, 11122.

2·Co change somewhat as the temperature decreases (see Table S2 of the Supporting Information). The structural change with varying temperature, although a little slight, should be one reason for the uncommon magnetic behavior. After reaching a minimum of 0.356 $cm^3\ mol^{-1}$ K at 18 K, $\chi_M T$ increase slightly to a maximum of 0.363 $cm^3\ mol^{-1}$ K at 14.5 K, indicating the possibility of weak ferromagnetic behavior due to the spin-canting. Upon further cooling, $\chi_M T$ drops sharply, suggesting AF interactions between the chains or the saturation effect in **2·Co**. A value of χ_M from 210 to 300 K obeys the Curie−Weiss law with a Curie constant $C = 3.48\ cm^3\ mol^{-1}$ K and a Weiss constant $\theta = -40.0$ K. The negative θ suggests an AF interaction between the Co^{2+} ions.

To further clarify the magnetic behavior, the temperature dependencies of the zero-field-cooled (ZFC) and the field-cooled (FC) magnetization were measured at a low field of 20 Oe (Figure 5a, inset). The obvious divergence of the ZFC and FC plots below 12.5 K indicates irreversibility resulting from the formation of a LRO of ferromagnetic-like ordered state.

We have also measured the temperature dependencies of ac magnetic susceptibility under $H_{dc} = 0$ Oe and $H_{ac} = 3$ Oe, with frequencies of 10 and 1000 Hz from 2 to 21 K (Figure S7, Supporting Information). The in-phase ac signal presents a peak at 12.4 K and confirms the occurrence of a phase transition, consistent with the temperature dependency data of dc susceptibility. The ac susceptibility exhibits an out-of-phase signal peak, which is in agreement with the occurrence of divergence of the ZFC and FC magnetizations, confirming the existence of spontaneous magnetization behavior. No frequency dependence of the ac signals was observed.

The isothermal magnetization with a field up to 50 kOe at 2.0 K is shown in Figure 5b. The initial increase of magnetization is relatively rapid and not linear with the field up to 8 kOe, and then it becomes almost linear with a smaller slope up to 0.084 Nβ per Co^{2+} at 50 kOe, far from the experimental saturation value of the Co^{2+} ion, suggesting the overall AF coupling between Co^{2+} ions. A hysteresis loop is observed clearly when the field is less than 10 kOe, giving a coercive field of $H_c \approx 500$ Oe and a remnant magnetization of $M_r = 0.0024$ Nβ.

According to the above magnetic measurements of the compound **2·Co**, we can draw a conclusion that **2·Co** is a spin-canted weak ferromagnet, and the canting angle is estimated to be about 0.063° based on the equation $\sin\theta = M_r/M_s$, where M_s is the saturation magnetization (at 2 K, the effective spin is $S = 1/2$ with a common value of g about 4.3 for Co(II)).[25] As we know, the spin-canting behavior is due to the single-ion magnetic anisotropy or antisymmetric interactions.[26] For **2·Co**, its structure revealed the presence of an inversion center between the bridged Co^{2+} sites, which forbids the occurrence of antisymmetric interactions. The spin-canting behavior of **2·Co** should be attributed to the single-ion anisotropy of Co(II) ions[27] or a possible structure phase transition at low temperatures, which will provides merit for future investigations. The role of the great single-ion anisotropy of Co(II) for the spin-canting behavior is similar to that of the compounds reported, such as $[Co_4(pico)_4(4,4'\text{-bpy})_3(H_2O)_2]_n \cdot 2nH_2O$, $\{[Co_3(hpdc)_2(H_2O)_6]\cdot 2H_2O\}_n$, Rb-$MnO_2$, and so forth.[27]

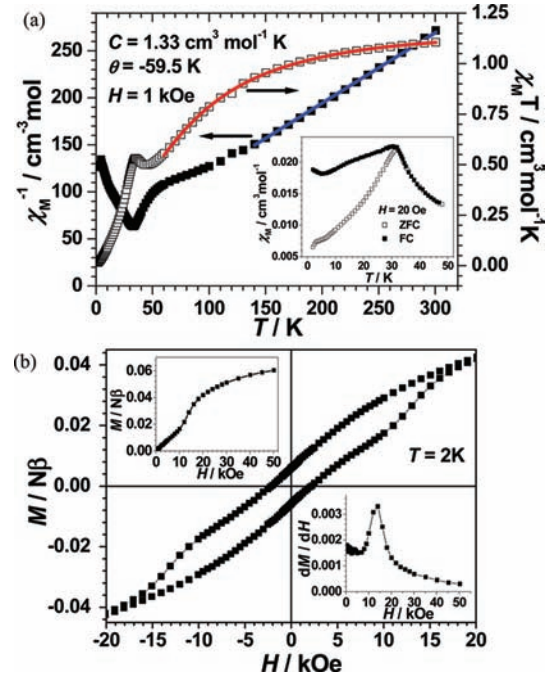

Figure 6. (a) The plots of $\chi_M T$ and χ_M^{-1} vs T for **3·Ni** at $H = 1$ kOe from 2.0 to 300 K. The blue solid line is the best fitting to the Curie−Weiss law, and the red one is the fit to the alternating chain model. Inset: The ZFC−FC plot of **3·Ni** at $H = 20$ Oe. (b) The hysteresis of 3·Ni at 2.0 K. Inset: The $M-H$ and dM/dH plot.

3·Ni. The magnetic properties of **3·Ni** are shown in Figure 6. The $\chi_M T$ value at 300 K is 1.10 $cm^3\ mol^{-1}$ K and decreases upon cooling, reaching 0.500 $cm^3\ mol^{-1}$ K at 44 K, and then increases to 0.532 $cm^3\ mol^{-1}$ K at 35 K. Upon further cooling, $\chi_M T$ drops sharply, suggesting AF interactions between the chains or the saturation effect. The upturn of $\chi_M T$ below 44 K suggests an uncompensated magnetic moment of the system possibly arising from spin canting of the antiferromagentically coupled Ni(II) ions. Fitting the data above 130 K with the Curie−Weiss law, we find $C = 1.33$ $cm^3\ mol^{-1}$ K and a negative Weiss constant $\theta = -59.5$ K, which indicates the dominant AF coupling between Ni^{2+} ions.

There are two types of exchange interactions, J_1 through the double EE-N_3 bridges and J_2 through the 3-fold bridges.

(25) Wang, X. Y.; Wang, Z.-M.; Gao, S. *Inorg. Chem.* **2008**, *47*, 5720.
(26) (a) Carlin, R. L. *Magnetochemistry*; Springer-Verlag: Berlin, 1986; Chapter 6. (b) Dzyaloshinsky, I. *J. Phys. Chem. Solids* **1958**, *4*, 241. (c) Moriya, T. *Phys. Rev.* **1960**, *117*, 635; **1960**, *120*, 91.
(27) (a) Zeng, M.-H.; Zhang, W.-X.; Sun, X.-Z.; Chen, X.-M. *Angew. Chem.* **2005**, *117*, 3139. (b) Jia, H.-P.; Li, W.; Ju, Z.-F.; Zhang, J. *Chem. Commun.* **2008**, 371. (c) Authier, A. *International Tables for Crystallography*; Kluwer Academic Publishers: Dordrecht, The Netherlands, 2003; Volume D: Physical Properties of Crystals, pp 127−132. (d) Pfeiffer, S.; Jansen, M. *Z. Anorg. Allg. Chem.* **2007**, *633*, 2558. (e) Wyrzykowski, D.; Warnke, Z.; Kruszyński, R.; Kłak, J.; Mroziński, J. *Trans. Metal Chem.* **2006**, *31*, 765.

We use a Heisenberg model[28] of an alternating one-dimensional AF/F chain with $S = 1$ to estimate the values of J_1 and J_2. The Hamiltonian is written as

$$H = -2\sum_{i=1}^{N-1} [J_1 S_{2i} S_{2i+1} + J_2 S_{2i} S_{2i-1}] \quad (2)$$

where $2N$ corresponds to the number of interacting spins and the negative J value refers to an AF coupling. The magnetic susceptibility of the AF/F alternative Heisenberg chain with $S = 1$ is a function of the exchange alternation parameter $\alpha = J_2/|J_1|$.

$$\chi_M = \frac{2Ng^2\beta^2}{3|J_1|}\chi_r \quad (3)$$

$$\chi_r = \frac{AT_r^3 + BT_r^2 + CT_r + D}{T_r^4 + ET_r^3 + FT_r^2 + GT_r + H} \quad (4)$$

$$T_r = \frac{kT}{|2J_1|} \quad (5)$$

where the expressions A∼H are the functions of α as follows, $X_i(\alpha) = x_0 + x_1\alpha + x_2\alpha^2 + x_3\alpha^3 + x_4\alpha^4 + x_5\alpha^5$, and the coefficients of x_i are given in the referred to paper. The best fitting for the data of 60 to 300 K gives $J_1 = -23.3$ cm^{-1}, $\alpha = J_2/|J_1| = 0.855$, $J_2 = +19.9$ cm^{-1}, $g = 2.16$ with $R = 1.8 \times 10^{-5}$, and $R = \sum(\chi_{obsd} - \chi_{calcd})^2/\sum(\chi_{obsd})^2$. The values of J_1 and J_2 indicate an AF coupling through the EE-N_3 bridge and a FO coupling through the 3-fold bridge. The former is consistent with the values through the same bridges reported in the literature.[3−8]

ZFC and FC plots measured in a low field of 20 Oe show obvious bifurcation at ca. 32 K with the decreasing temperature (Figure 6a, inset). This behavior may arise from the onset of LRO. The slight increase below 5 K maybe result from a trace amount of paramagnetic impurities. The zero-field ac magnetic susceptibility with frequency $f = 10$, 100, and 1000 Hz was measured under $H_{dc} = 0$ Oe and $H_{ac} = 3$ Oe from 2.0 to 48 K (Figure S8, Supporting Information). The in-phase signals show a peak at ca. 32.5 K, and the occurrence of the nonzero out-of-phase signal indicates that there exists a spontaneous magnetization below 34 K. No obvious frequency dependence of the ac signals was observed.

The field-dependent magnetization of **3·Ni** shows a pronounced sigmoid shape, indicating the occurrence of a magnetic transition induced by the external field (Figure 6b). The transition field, determined by a dM/dH derivative curve, is ca. 14 kOe. The magnetization at 50 kOe is 0.06 Nβ for each Ni(II) ion, much lower than the expected saturation value of 2.0 Nβ anticipated for $S = 1$ spins with $g = 2.0$, suggesting the overall AF couplings between Ni(II) ions. A hysteresis loop is observed clearly at 2.0 K giving a coercive field of $H_c \approx 2.2$ kOe and a remnant magnetization of $M_r = 0.0060$ Nβ.

According to the above magnetic measurements, compound **3·Ni** displays spin-canted AF behavior, which may originate from the single-ion anisotropy of Ni(II) and possible structural phase transition, since the occurrence of antisymmetric or $D-M$ interaction is forbidden because of the presence of an inversion center between Ni ions in **3·Ni** with space group $P\bar{1}$.[27] The origin of the spin-canting behavior of **3·Ni** is similar to that of **2·Co**. The canting angle is estimated to be about 0.17°. Compared to **5**, the introduction of an acetate group in **3·Ni** does not affect remarkably the exchange interactions between Ni(II) ions but changes the topology of the chain, thus bringing on the spin-canting behavior in **3·Ni**.

Conclusion

In conclusion, by introduction of the flexible bidentate blocking ligand dpa, three 1D azide-bridged Cu(II), Co(II), and Ni(II) coordination polymers have been synthesized and characterized structurally and magnetically. Due to the flexibility of dpa, a series of different chain structures was obtained. For Cu(II), the metal ions are linked by single EO-N_3 to form a uniform chain while another azide acts as the terminal ligand. For Co(II), the metal ions are connected by double EO-N_3 and double EE-N_3 to form an alternative chain. A type of novel 3-fold bridge is found in the Ni(II) compound, which is composed of two EO-N_3 and one acetate group. The 3-fold bridges link the neighboring Ni(II) ions to form nickel dimers, and then the dimers are connected by EE-N_3 to afford the alternative chain structure. In complex **1·Cu**, overall AF exchange interactions are observed, and no long-range ordering exists above 2.0 K. Complexes **2·Co** and **3·Ni** behave as spin-canted weak ferromagnets with $T_N = 12.4$ and 32.5 K, respectively. This work demonstrates that azide is a versatile bridging ligand to construct molecule-based magnets, and the combination of azido and flexible coligands could result in varied lower dimensional structures, which is expected to provide more novel model compounds with which to investigate fascinating magnetic behaviors.

Acknowledgment. This work was funded by the National Science Fund of China (Grants 20821091, 20490210, and 20571005) and the National Basic Research Program of China (Grant 2006CB601102).

Supporting Information Available: CIF files, plots of crystal packing, more figures of magnetic data, and selected bond lengths and angles for the compounds. This material is available free of charge via the Internet at http://pubs.acs.org.

IC801505A

(28) (a) Borras-Almenar, J. J.; Clemente-Juan, J. M.; Coronado, E.; Lloret, F. *Chem. Phys. Lett.* **1997**, *275*, 79. (b) Miller, J. S.; Drillon, M. *Magnetism: Molecules to Materials I*; Wiley-VCH: Weinheim, germany, 2005; Chapter 1.